Journal of the Nigerian Association of Mathematical Physics
***Volume* 19 (November, 2011), pp 205 – 210**

Potentially Induced Artificial Heat Reservior

[1]Onimisi M. Y. and [2]Okoro C. I.

Department Of Physics,
Nigerian Defence Academy, P.M.B 2109, Kaduna, Nigeria.

Abstract

When heat flow is subject to temperature dependent thermal potential, the associated local temperature field is significantly influenced. This response exhibits interesting effects. This paper examines these effects over a hexagonal plate (fig.2). A linear thermal potential is induced at the boundary and finite element algorithm employed to compute the temperature profiles. A control model is set-up and the outputs from the test model and the control model are examined and compared. Our results show that the temperature field due to the linear potential exhibits artificial heat reservoirs at localized node due to the concentration of the potential. These heat reservoirs are invaluable in the optimum design economy of thermally driven systems.

Keywords: Thermal potential; Control model; Heat reservoir; Finite element algorithm; Thermal interactions.

1. Introduction

The response of temperature field to any external thermal field is best understood at the molecular level. The original heat profile is significantly influenced by the particular form of induced potential at the boundary. In idealized models, these external thermal fields, according to the cause effect theory, must cause significant changes to the system under study. Such changes yield certain effects which require qualitative treatments, either by laboratory experiments or by computer simulations.

Common thermal potentials have been used in the simulation of heat flow problems. Non-linear temperature dependent potentials have been used to demonstrate thermal shape sensitivity [1] and convection thermal potential has been used as boundary formulation to study internal point sensitivity [2]. Effects resulting from these thermal responses have also been studied. Strong non-linearity has been observed due to viscous dissipation [3] and also on solids [4, 5]. In a recent thesis [6], the control temperature limits have been observed to be altered significantly, depending on the form of the potential and simulation data, from a study of linear, radiation and logarithmic potentials at the boundary.

Understanding of heat flow problems plays significant role in the design and economy of most systems such as in nuclear power plants, thermo-chemical plants and thermo-mechanical industries. Results obtained from heat reservoir for real absorption heat transformer provide some guidance for the optimum design of absorption heat transformer [7]. Absorbed heat can be released back to the ambient via a heat rejection subsystem. This results in heat sinks which decrease cost and noise, and increasing reliability [8].These systems have been understood, mostly, from quantitative analysis. Little effort is been put in the computer simulation of such systems.

Obviously, the efficiency of heat engines depends on the temperature range of the system. This efficiency increases with increase in the temperature difference between the hot reservoir and cold reservoir. The ground, as a source of heat pump systems and as a loop heat exchanger, has been demonstrated to be efficient [9]. In this model, the heat pump is divided into heating and cooling components to allow connection to both heating and chilled water plant loops. So-to-speak, the design methodology of such systems must incorporate thermal interactions with induced external fields.

In this work, we demonstrate the use of computer facilities in simulation of heat reservoir and demonstrate heat reservoirs as effects caused by induced thermal potential at the boundary.

NOMENCLATURE

A Area, m**2
A_i Area of ith element, m**2
B^e Temperature gradient interpolation matrices
E Surface emissivity, dimensionless
G Arbitrary functional

Corresponding authors: E-mail: - , Tel. +2348054538199/+2348065696431

H Point heat source, W/ m**3/sec
H^e Generalized element temperature
h Thermal conductivity, J/sec/m/K
J^e Element Jacobian
κ Thermal diffusivity, m**2/sec.
M Parameter specifying real coefficient
N_i Shape function of ith node
$\boldsymbol{N_e^n}$ Element shape function for node n, element e
Q Extended heat source, W/ m**3/sec.
$\boldsymbol{Q_p}$ Point heat source, W/ m**3/sec.
$\boldsymbol{R_e}$ External source, , W/ m**3/sec.
S Parameter specifying real coefficient
r,s Natural coordinates
t Time, sec.
T Temperature field, K.
$\bar{T}$ Temperature derivative with respect to time, K/sec
u,v Parametric coordinates
x, y Cartesian coordinates

1. THE MATHEMATICAL MODEL

We consider an arbitrary volume V lying within the solid plate and bounded by a surface S as shown below.

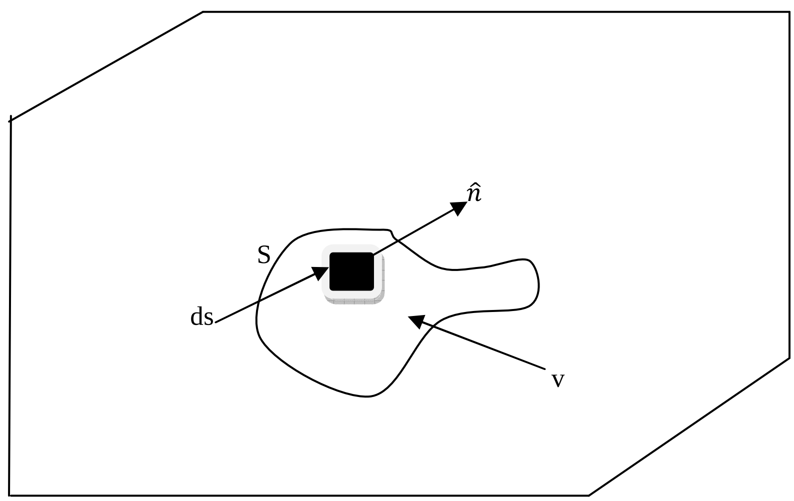

Fig.1: Arbitrary volume V bounded by the surface S.

For steady state flow in the presence of heat sources, the heat flow is modeled as the familiar 2-dimensional Poisson's equation:

$$\nabla^2 T = \frac{1}{k}(Q + Q_p \delta(r - r_p)) \tag{1}$$

2. FORMULATION OF NUMERICAL ALGORITHM

We now seek to derive the 2D finite element scheme for equation (1) from which the temperature field evolves within the minimum computational error.

Consider the minimization problem:

$$dI = \int_A \left(\frac{\partial G}{\partial T}\, dT + \frac{\partial G}{\partial \bar{T}} d\bar{T}\right) \mathrm{dA} = 0 \tag{2}$$

The general functional for the 2-dimensional heat flow is

$$\mathrm{G}(\mathrm{x}, \mathrm{y}, T, \bar{T}) = \frac{1}{2}\sigma\left[\left(\frac{\mathrm{dT}}{\mathrm{dy}}\right)^2\right] - \frac{1}{2}\mathrm{HT}^2 + \frac{1}{\mathrm{k}}\mathrm{QT} \tag{3}$$

$$\frac{\partial G}{\partial T} = -HT + \frac{1}{\mathrm{k}}\mathrm{Q} \;\; ; \frac{\partial G}{\partial \bar{T}} = \sigma \frac{\mathrm{dT}}{\mathrm{dy}} \tag{4}$$

Putting these derivatives into equation (2) gives;

$$dI = \int_{S_1}^{S_2} \left(-HT + \frac{1}{\mathrm{k}}\mathrm{Q}\right) dT \mathrm{dS} + \int_{S_1}^{S_2} \sigma \frac{\mathrm{dT}}{\mathrm{dy}}\;\; d\bar{T}\mathrm{dS} \tag{5a}$$

$$\lim_{\Delta x \Delta y \to 0} dA = dS \tag{5b}$$

Using integration by parts on the second integral in equation (5a) and then integrating the resulting differential we obtain

$$I = \iint_A \frac{1}{2}\sigma\nabla^2 T dA + \int_S \frac{1}{2}HT^2 dS - \iint_A \frac{1}{k}QTdA \quad (6)$$

For some edge S over which the plate thermally interacts with the surrounding.

In an effort to develop the finite element model, a linear interpolation was considered and an appropriate shape function has been chosen.

$$N_i = \frac{A_i}{A}, \text{ i=1,2,3} \quad (7)$$

Since element strains are obtained by taking the derivatives with respect to the Cartesian coordinates, we have the following relations;

$$x = \sum_{i=1}^{3} N_i\, x_i\ ,\ y = \sum_{i=1}^{3} N_i\, y_i,\ x = \sum_{i=1}^{3} h_i\, x_i\ ,\ y = \sum_{i=1}^{3} h_i\, y_i,\ u = \sum_{i=1}^{3} h_i\, u_i\ ,\ v = \sum_{i=1}^{3} h_i\, v_i$$

$h_1 = 1 - r - s, h_2 = r, h_3 = s,$ provided$\sum_{i=1}^{3} h_i = 1$. The evaluation of the element matrices now involves a Jacobian transformation and all integrations carried out on the natural coordinates, i.e. r's integrations go from 0 to 1 and the s integrations go from 0 to (1-r).The Jacobian, generalized element temperature and the temperature-gradient interpolation matrices, respectively are;

$$J^e = \begin{pmatrix} \frac{\partial x}{\partial r} & \frac{\partial y}{\partial r} & \frac{\partial z}{\partial r} \\ \frac{\partial x}{\partial s} & \frac{\partial y}{\partial s} & \frac{\partial z}{\partial s} \\ \frac{\partial x}{\partial t} & \frac{\partial y}{\partial t} & \frac{\partial z}{\partial t} \end{pmatrix} \quad (8)$$

$$H^e = \begin{pmatrix} h_1 & 0 & h_2 & 0 & h_3 & 0 \\ 0 & h_1 & 0 & h_2 & 0 & h_3 \end{pmatrix} \quad (9)$$

$$B^e = \begin{pmatrix} \frac{\partial h_1}{\partial x} & 0 & \frac{\partial h_2}{\partial x} & 0 & \frac{\partial h_3}{\partial x} & 0 \\ 0 & \frac{\partial h_1}{\partial y} & 0 & \frac{\partial h_2}{\partial y} & 0 & \frac{\partial h_2}{\partial y} \\ \frac{\partial h_1}{\partial y} & \frac{\partial h_1}{\partial x} & \frac{\partial h_2}{\partial y} & \frac{\partial h_2}{\partial x} & \frac{\partial h_3}{\partial y} & \frac{\partial h_3}{\partial x} \end{pmatrix} \quad (10)$$

Thus the element stiffness matrix is computed as

$$K^e = \text{h}\iint B^{(e)T} C B^e det.J^e dA \quad (11)$$

The extended heat source, the differential boundary condition and the point sources are computed respectively as;

$$R_Q^e = \text{h}\iint H^{(e)T} Q det.J^e dA; \quad (12)$$

$$R_S^e = \int_S H^{(e)T} \frac{\partial T}{\partial n} det.J^e ds\ ; \quad (13)$$

$$R_p^e = \sum_i H^{(e)T} Q_p \frac{T_p}{k} \quad (14)$$

Using the principle of virtual temperature and assembling the element matrices we obtain the general finite element scheme;

$$\text{KT} = R_Q + R_S + R_P \quad (15)$$

3. THE TEST CASE

Our test plate was modeled with 34 nodes and 48 triangular elements spanning the entire domain as shown in fig.2. We have also considered point source of strength 2×10^5 situated at nodes 7 and 30. A uniform extended source of strength 10^6 has been applied. The potential is applied at nodes 17, 24 and 31. The following data was used in the computation:

- A=0.02; ; $\text{Q}_\text{p} = 2 \times 10^5$; $\text{Q} = 10^6$; $\kappa = 2 \times 10^3$; $S = 4.5 \times 10^4$ ds=0.2;M=-15; $|J|$=0.04

4. RESULTS AND DISCUSSION

We have employed the finite element algorithm on the test case. The response of the model to the linear potential has been computed. The simulation graphs were generated using MATLAB 7.5.0 graphic features with a Window XP operating system. In order to assess the effects, we have also computed the control model by simply setting the right hand of (15) to zero, thereby solving a typical Laplace's problem. The numerical results are tabulated in table1.

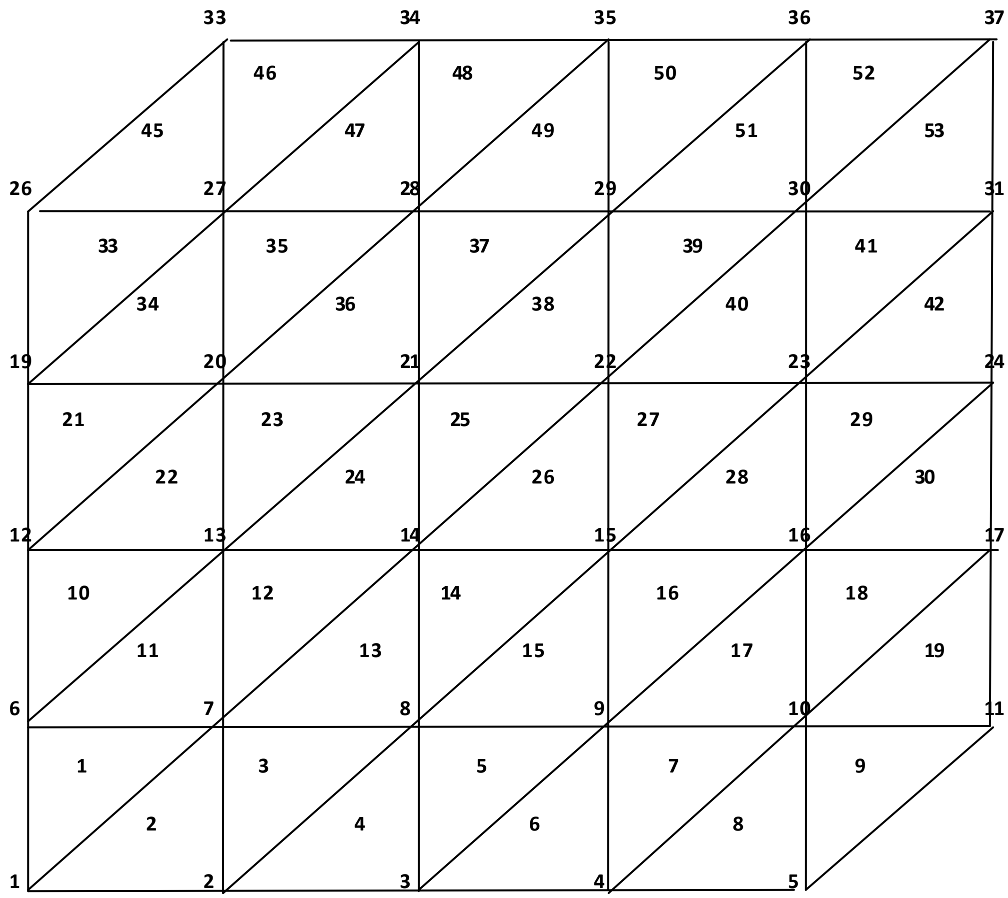

Fig.2: The finite element discretization of the simulation plate

Table1: **NUMERICAL RESULTS**

NODE TEMPERATURE (K)

	LINEAR	CONTROL
1	750.00	750.00
2	800.00	800.00
3	800.00	800.00
4	800.00	800.00
5	800.00	800.00
6	700.00	700.00
7	700.75	712.50
8	801.71	741.67
9	800.75	749.67
10	790.00	700.00
11	750.00	750.00

12	700.00	700.00
13	734.45	708.33
14	821.29	739.42
15	821.54	739.42
16	742.84	749.20
17	699.94	747.30
19	700.00	700.00
20	734.42	708.33
21	804.06	733.34
22	809.97	738.78
23	760.56	742.82
24	714.73	741.55
26	700.00	700.00
27	706.38	697.35
28	597.06	714.55
29	597.04	724.44
30	597.66	660.77
31	483.45	680.33
33	500.00	500.00
34	500.00	500.00
35	500.00	500.00
36	500.00	500.00
37	600.00	600.00

- **DISCUSSION OF RESULTS**

Inducing the linear thermal potential at the boundary on the hexagonal plate has yielded results quite interesting. The temperature limits for the control model (Fig.3) have been significantly deviated as exhibited by the test model (Fig.2). The deviations from the lower limit temperature at node 31 and the upper limit temperature at nodes 14 and 15 (Table 1) are due to the induced potential. The internal nodes (14 and 15) also respond to the induced boundary potential. These deviations are interpreted as induced global maximum for the upper limit and global minima for the lower limit which imply hot and cold heat reservoirs.

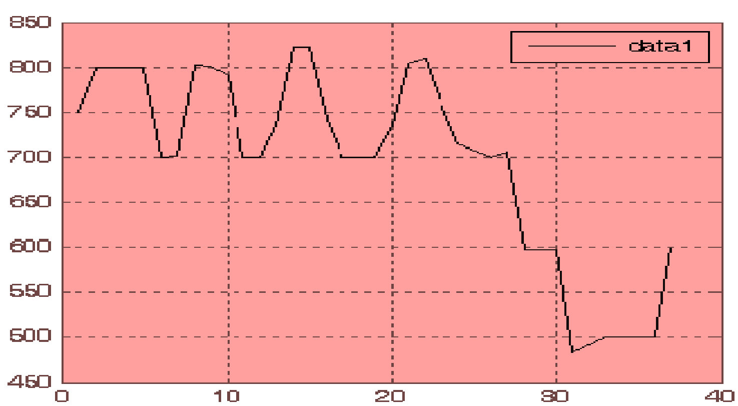

Fig.2:Temp.(K) VS Node number for the test model.

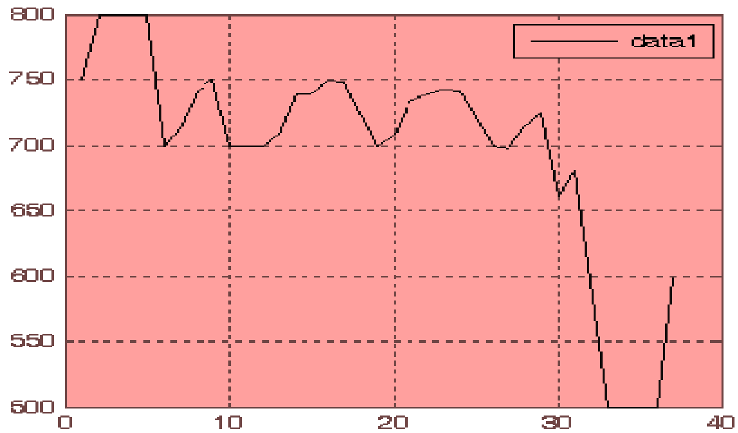

Fig.3: Temp.(K) VS Node number for the control model.

1. CONCLUSION

In this paper, we studied the response of heat flow profiles to temperature dependent boundary formulation. The influence of the linear thermal potentials has been examined. The temperature profiles for the test model, in comparison to the control model, show that the evolution of the temperature field depends on the boundary formulation. It could be observed that these deviations are caused by the induced potential. This shows that the global extremities are artificially induced heat reservoirs (source and sink). These heat reservoirs are, thus, essential design factors for the operation of thermally driven systems.

REFERENCES

[1] Prasad, K.G. and Kane, J.H. (1992): 3D Boundary Element Shape Sensitivity Analysis, International Journal for Heat and Mass Transfer, 35/6: pp.1427-1439.

[2] Kane, J.H. and Wang, H. (1991): Boundary Element Shape Sensitivity Analysis Formulations for Thermal Problems with Non-Linear Boundary Conditions, AIAA Journal, vol.29, no.5.

[3] Massoudi,M; Trad, P.X. and Wulandana, R.(2009): Convective-Radiation Heat Transfer in a Non-Linear Fluid With Temperature Dependent Viscosity, Journal of Mathematical Problems in Engineering vol. 2009, Article id 232670,doi: 10.1155/2009/232670, Hindawi Publishing Corporation.

[4] Bialecki, R. and Nawak, A.J. (1950): Boundary Value Problems for Non-linear Material and Non-linear Boundary Conditions, Applied Mathematics Modeling 5, pp.417-421

[5] Onishi, K. and Kuroki, T. (1982): Boundary Element Method in Singular and Non-Linear Heat Transfer in Brebbia, c(Ed): Boundary Element Methods in Engineering, Berlin, Springer-Verlag: pp. 141-155

[6] Okoro C.I. (2011): Finite Element Modeling and Simulation of Some Observable Effects of Heat Flow Response to Boundary Formulation, MSc. Thesis (unpublished), Dept. of Physics, Nigerian Defence Academy, Kaduna, Nigeria.

[7] Chen, L.; Qin, X. and Sun, F.: Model of Irreversible Finite-Heat Capacity Heat Reservoir Absorption Heat Transformer Cycle and its Application, SAGE Journals.

[8] Enertron Incorporation: Phase-Change Heat Reservoir Device for Transient Thermal Management, Chandler, US.

[9] Fisher E.D. and Rees S.J. (2005): Modeling Ground Source Heat Pump Systems in a Building Energy Simulation Program (ENERGYPLUS), 9th International IBPSA conference, Canada.